

## Equivalence of *trans* paths in ion channels

Juan Alvarez\*

*Mathematical Sciences Group, University of Saskatchewan, 142 McLean Hall, 106 Wiggins Road, Saskatoon, SK, Canada S7N 5E6*

Bruce Hajek<sup>†</sup>

*Department of Electrical and Computer Engineering and the Coordinated Science Laboratory,  
University of Illinois at Urbana-Champaign, 1308 West Main Street, Urbana, Illinois 61801, USA*

(Received 12 January 2006; published 21 April 2006)

We explore stochastic models for the study of ion transport in biological cells. Analysis of these models explains and explores an interesting feature of ion transport observed by biophysicists. Namely, the average time it takes ions to cross certain ion channels is the same in either direction, even if there is an electric potential difference across the channels. It is shown for simple single ion models that the distribution of a path (i.e., the history of location versus time) of an ion crossing the channel in one direction has the same distribution as the time-reversed path of an ion crossing the channel in the reverse direction. Therefore, not only is the mean duration of these paths equal, but other measures, such as the variance of passage time or the mean time a path spends within a specified section of the channel, are also the same for both directions of traversal. The feature is also explored for channels with interacting ions. If a system of interacting ions is in reversible equilibrium (net flux is zero), then the equivalence of the left-to-right *trans* paths with the time-reversed right-to-left *trans* paths still holds. However, if the system is in equilibrium, but not reversible equilibrium, then such equivalence need not hold.

DOI: [10.1103/PhysRevE.73.046126](https://doi.org/10.1103/PhysRevE.73.046126)

PACS number(s): 02.50.-r, 87.16.Uv, 02.70.Ns, 82.39.Wj

### I. INTRODUCTION

A biological cell interacts with its surrounding medium through its membrane, which acts as gatekeeper between the interior and exterior of the cell. The membrane is a lipid bilayer that is essentially impermeable to ions, so that the transport of ions between the interior and exterior of the cell takes place through channels formed by proteins. The transport of ions through these channels plays an important role in the function of the cells and hence in many processes of biological interest. Ions diffuse and drift through an aqueous pore as they move from a bath of one concentration to a bath of another concentration. Ions diffuse from regions of high concentration to regions of low concentration according to Fick's law [1,2] in the absence of electric fields. They drift due to electric fields caused by fixed charges in the channel walls, charges from the other ions in the channel, the dielectric properties of the channel, and the transmembrane potential, according to Ohm's law [1,2].

The modeling of ion transport in solutions through channels is an area of intense research due to its complexity and importance. Among the most common approaches in this area one can find molecular dynamic simulations [3–8], Brownian dynamics simulations [3–13], reaction-rate models [2,3,14,15], and Nernst-Planck (NP) electrodiffusion models [2–5,7,8,14–18]. This paper uses discrete-state models for a one-dimensional channel, along the lines of both the reaction-rate and NP electrodiffusion theories, to represent the dynamics of ion diffusion across a channel between two baths.

The main focus of this paper is a symmetry between ions traversing a channel in one direction and ions crossing in the other direction, both for isolated ions and for interacting ions. We first discuss the symmetry property in the simplest model: that of a single-ion channel in discrete time and discrete space. The details are simplified by the fact that each individual *trans* path has a positive probability in such a model. Single-ion models are applicable to systems where the concentrations are low enough that there is usually at most one ion inside the channel at any given time or to single-ion occupancy channels like the gramicidin channel [19]. The models in this family also serve as building blocks for models with multiple ions. We then turn our attention to models with multiple interacting ions. There we use a discrete-space continuous-time model. The use of discrete space permits analysis and simulation, while the use of discrete time avoids issues associated with ions simultaneously making discrete jumps.

Although our analysis is done for discrete-space models in both discrete and continuous time, the physical laws that govern the channel are fundamentally continuous in nature. Thus, we use discrete-state models that, in the limit of small step size, converge to continuous-state models. Special interest is paid to preserving time-symmetry properties that may be present in continuous-state models, to the discrete-state models. The space discretization is done by dividing the channel into  $N$  sites labeled  $1, \dots, N$  and considering the left and right baths as sites  $0$  and  $N+1$ , respectively. Figure 1 depicts this discretization. At any given time, ions can be located in the channel or in either one of the baths, but they cannot be located in the membrane because the membrane is assumed impermeable to ions. Models can be closed or open. Closed models include the channel and baths, so ions remain in the system forever. Open models include the channel but

\*Electronic address: [jalvarezv@ieee.org](mailto:jalvarezv@ieee.org)

<sup>†</sup>Electronic address: [b-hajek@uiuc.edu](mailto:b-hajek@uiuc.edu)

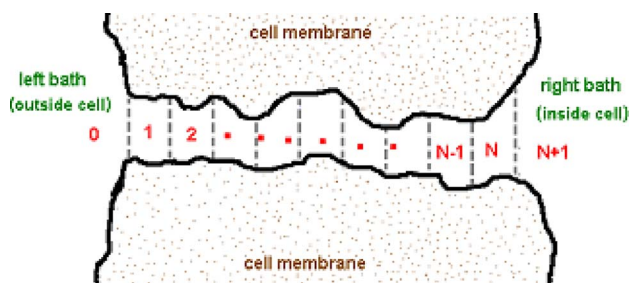


FIG. 1. (Color online) Discrete-space model.

not the baths, so ions are killed when they reach the baths. We study Markov models of an ion channel in this paper, although there is growing evidence that ion channels cannot be accurately modeled by Markov processes. See the discussion in Sec. VIII. An excellent description of the theory of symmetry and reversibility for discrete-state processes is given by Kelly [20], which includes applications to migration processes, population genetics, and queueing systems. Additional references for symmetric diffusions are given in Sec. IV.

The remainder of the paper is organized as follows. Section II describes the discrete-space, discrete-time models for a single-ion, and Sec. III proves the symmetry property for the single-ion model. Sections IV–VI lay the groundwork for examining the time symmetry of *trans* paths for an interacting ion model. Section IV relates discrete-state models to continuous-state models. Section V begins the description of models with multiple ions by working under the assumption of no interaction among the ions and expressing the equilibrium distribution of an open channel as a grand canonical ensemble. This viewpoint, which is grounded in statistical physics, is exploited in Sec. VI to help motivate the model for interacting ions. With this foundation, Sec. VII examines the question of symmetry in an open-channel model with interacting ions in equilibrium.

## II. DISCRETE MODELS FOR SINGLE-ION MOTION

This section considers two related discrete-time Markov chain models for single-ion motion. The models can be easily adapted to obtain continuous-time models. First, consider a closed model, such that the location of the ion is represented by a discrete time Markov chain  $X$  on sites  $0, \dots, N+1$ .

For  $i, j \in \{0, \dots, N+1\}$ , the transition probability  $p_{i,j}$  is the probability the ion is at site  $j$  after one time step, given that it is at state  $i$  at the beginning of the time step. Assume that  $p_{i,j} = 0$  for  $j \notin \{i-1, i, i+1\}$  and that  $p_{i,j} > 0$  whenever  $|i-j| = 1$ . Also assume that  $\sum_j p_{ij} = 1$  for each  $i$ , so that the Markov chain is conservative (i.e., the total probability mass is 1 at any time). This type of Markov chain is depicted in Fig. 2 and is known as a *birth-death process*. The drift of this process in state  $i$  is given by  $p_{i,i+1} - p_{i,i-1}$ . The selection of transition probabilities to match diffusion coefficients and electric potentials (including the effect of induced surface charges on the dielectric channel boundary) of physical channels is discussed in Sec. IV.

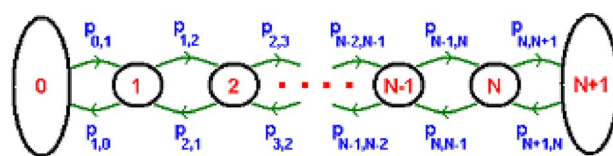


FIG. 2. (Color online) Conservative birth-death process on  $\{0, \dots, N+1\}$ . Self-loops are omitted.

Next, consider a related open model, such that the location of the ion is represented by a discrete-time Markov chain  $\hat{X}$  on  $1, \dots, N$  killed at the boundaries. Suppose that the one-step transition probabilities  $p_{i,j}$  are the same as those for the closed model for  $i = 1, \dots, N$ . Therefore  $\hat{X}$  is a birth-death process killed at the boundaries, and it is depicted in Fig. 3. Given that the ion is at state 1 at some time  $k$ , the ion next jumps towards state 0 with probability  $p_{10}$  and vanishes, in which case the Markov process is said to be killed at time  $k+1$ . Therefore, the process is not conservative.

## III. EQUIVALENCE OF *trans* PATH DISTRIBUTION

The model described in Sec. II induces a probability distribution on the set of left-to-right *trans* paths and another probability distribution on the set of right-to-left *trans* paths. In this section these distributions are shown to be equivalent under time reversal. The equivalence holds for arbitrary potential profiles, which can include the effect of induced surface charges, for continuous time and state, as well as for closed models. A key to the proof is a concept of symmetry, related to the notion of reversibility, of Markov processes.

Consider the open model described in Sec. II. Let  $\gamma = (\gamma_0, \dots, \gamma_m)$  be a path of finite length  $m$ , where  $\gamma_b \in \{1, \dots, N\}$  for  $b \in \{0, \dots, m\}$  and  $|\gamma_b - \gamma_{b-1}| \leq 1$  for  $b \in \{1, \dots, m\}$ . A *trans path* is a path that starts at a boundary and ends at the other boundary. Let  $\mathcal{S}_{LR}$  be the set of left-to-right *trans* paths, consisting of all paths  $\gamma$  of the form

$$\gamma = (\gamma_0 = 1, \gamma_1, \dots, \gamma_{m-1}, \gamma_m = N),$$

where it is implicit that the ion jumps from the left bath into site 1 just before time 0 and that it jumps from site  $N$  to the right bath at time  $m+1$ . Similarly, let  $\mathcal{S}_{RL}$  be the set of right-to-left *trans* paths, consisting of all paths  $\gamma$  of the form  $\gamma = (\gamma_0 = N, \gamma_1, \dots, \gamma_{m-1}, \gamma_m = 1)$ . In this case, it is implicit that the ion jumps from the right bath into site  $N$  just before time 0 and that it jumps from site 1 to the left bath at time  $m+1$ .

For  $\gamma \in \mathcal{S}_{LR}$  let  $\tilde{\gamma}$  be the concatenation of  $\gamma$  and site  $N+1$ —i.e.,  $\tilde{\gamma} = (\gamma_0, \dots, \gamma_m, N+1)$ —and let  $P_{LR}[\gamma] := P^1[\tilde{\gamma} | T_{N+1} < T_0]$ , where  $T_0$  and  $T_{N+1}$  are the destruction

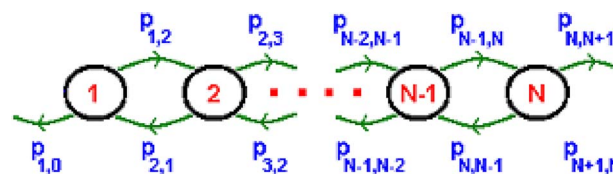


FIG. 3. (Color online) Birth-death process on  $\{1, \dots, N\}$  killed at the boundaries. Self-loops are omitted.

times at the left and right boundaries, respectively; e.g.,  $T_0$  is the time at which  $\hat{X}$  jumps from site 1 into the left bath, where it is immediately killed. Similarly, for  $\gamma \in \mathcal{S}_{RL}$ , let  $P_{RL}[\gamma] := P^N[\hat{\gamma} | T_0 < T_{N+1}]$  where  $\hat{\gamma}$  is the concatenation of  $\gamma$  and site 0.

For any finite path  $\gamma = (\gamma_0, \gamma_1, \dots, \gamma_{m-1}, \gamma_m)$ , define its time-reversed path  $\gamma_{rev} = (\gamma_m, \gamma_{m-1}, \dots, \gamma_1, \gamma_0)$ . Then,  $\gamma \in \mathcal{S}_{LR}$  implies that  $\gamma_{rev} \in \mathcal{S}_{RL}$  and vice versa. The mapping of  $\gamma \in \mathcal{S}_{LR}$  to  $\gamma_{rev}$  is a one-to-one and onto mapping of  $\mathcal{S}_{LR}$  to  $\mathcal{S}_{RL}$ . The symmetry equivalence result is stated as a proposition.

*Proposition III.1.* For any  $\gamma \in \mathcal{S}_{LR}$ ,  $P_{LR}[\gamma] = P_{RL}[\gamma_{rev}]$ . The proof of this proposition is provided in Appendix A. It is based on the detailed balance [20] or  $\mathcal{V}$  symmetry [21] of Markov chains.

Since  $\gamma$  in proposition III.1 is arbitrary and there is a one-to-one and onto mapping of  $\mathcal{S}_{LR}$  to  $\mathcal{S}_{RL}$ , the distribution of left-to-right *trans* paths is equal to the distribution of time-reversed right-to-left *trans* paths. This equivalence holds for arbitrary nonzero one-step transition probabilities of a birth-death process and can be extended to the continuous-state process obtained as the diffusion limit of this Markov chain [22] for arbitrary potential profiles.

The equivalence explains why the mean passage times obtained in [19] for channels with single-ion occupancy are symmetrical around zero transmembrane potential. The potential profile in [19] has two components: a linear component with slope  $\mu$  and a nonlinear component that is symmetrical around the center of the channel. A *trans* path from left to right when the linear component has slope  $\mu$  sees the same potential profile as the time-reversed *trans* path when the linear component has slope  $-\mu$ . Since the *trans* paths from right to left are equal in distribution to the time-reversed left-to-right *trans* paths for any potential profile, the *trans* paths from left to right when the linear component has slope  $-\mu$  are equal in distribution to those *trans* paths from left to right when the linear component has slope  $\mu$ . This observed symmetry of transit time distributions as a function of transmembrane potential around zero transmembrane potential relies on the assumption that the nonlinear component of the potential is symmetric about the center of the channel. However, the equivalence in distribution of the left-to-right *trans* paths and the time-reversed right-to-left *trans* paths holds for any potential profile.

The equivalence in distribution of the left-to-right *trans* paths and the time-reversed right-to-left *trans* paths also explains why the average translocation time in [23] does not depend on the direction in which the ion translocates. The result given here is stronger than the equivalence of mean passage times. It states that the distribution of these paths is equivalent when they are time reversed. For example, not only is the mean duration of these paths equal, but other measures, such as the variance of passage time or the mean time a path spends within a specified section of the channel, are also the same for both directions of traversal. This sounds counterintuitive at first, but it results from the fact that an ion that diffuses against a strong electric potential must do so quickly or else it will be much more unlikely to cross at all.

#### IV. MARKOV CHAINS ASSOCIATED WITH REVERSIBLE DIFFUSION PROCESSES

This section discusses symmetry and reversibility for diffusion processes and describes a space discretization procedure that preserves these properties. Space discretization enables easy computation and simulation, while preserving the symmetry of continuous-state models inherent in the underlying physical forces. As mentioned in the Introduction, this and the following two sections lay the groundwork for examining the time symmetry of *trans* paths for an interacting ion model, by progression from single-ion models in this section, to noninteracting ion models in the next section, to interacting ion models in the section after that.

For the purposes of this paper, it suffices to consider a one-dimensional diffusion, but the descriptions and procedures of this section apply to higher-dimensional processes as well, as described in Appendix B. Let  $B$  be an open connected subset of  $\mathbb{R}$ . A one-dimensional diffusion on  $B$  has a backwards generator which is a second-order differential operator of the form

$$\mathcal{L}\phi = D \frac{\partial^2 \phi}{\partial x^2} + \mu \frac{\partial \phi}{\partial x},$$

such that  $D$  is a positive-valued function on  $B$  and  $\mu$  is a real-valued function on  $B$ . The generator can be rewritten in a more symmetrical (as an operator) form as

$$\mathcal{L}\phi = \frac{\partial}{\partial x} D \frac{\partial \phi}{\partial x} + \tilde{\mu} \frac{\partial \phi}{\partial x},$$

where

$$\tilde{\mu} = \mu - \frac{\partial D}{\partial x}.$$

The function  $\mu$  specifies the infinitesimal drift of the process, and  $2D$  specifies the infinitesimal variance of the process.

In addition, the behavior of the diffusion at the boundary  $\partial B$  of  $B$  must be specified, unless the diffusion cannot reach the boundary, such as if  $B = \mathbb{R}$ . Following Kent [21], we shall assume that the boundary behavior is a mixture of destroying and normal reflection at the boundary. The boundary behavior is specified by the following condition for a function  $f$  on  $B$ :

$$\alpha f + \beta n \frac{\partial f}{\partial x} = 0 \quad \text{on } \partial B, \quad (1)$$

where  $\alpha$  and  $\beta$  are functions on  $\partial B$  with  $0 \leq \alpha \leq 1$  and  $\alpha + \beta \equiv 1$  and  $n(\xi)$  is the outward pointing normal vector at  $\xi \in \partial B$ . If  $\alpha \equiv 1$ , then the process is killed at the boundary and the process is not conservative. If  $\alpha \equiv 0$ , the process is reflected at the boundary and is therefore conservative.

Given a positive, twice continuously differentiable function  $v$  on  $B$ , the inner product of two functions  $\psi$  and  $\phi$  on  $B$  relative to  $v$  is defined as  $(\psi, \phi)_v = \int_B \psi \phi v dx$ . The adjoint operator of  $\mathcal{L}$  with respect to the inner product  $(\cdot, \cdot)_1$ , denoted by  $\mathcal{L}^*$ , corresponds to the spatial derivative component of the Smoluchowski diffusion equation—i.e.,  $\partial \phi / \partial t = \mathcal{L}^* \phi$  with  $\tilde{\mu} = -D\beta \partial u / \partial x$  and  $u(x)$  being the potential function.

The diffusion specified by  $\mathcal{L}$  and the boundary condition (1) is said to be symmetric with symmetry density  $v$ , or simply  $v$  symmetric, if  $(\mathcal{L}\psi, \phi)_v = (\psi, \mathcal{L}\phi)_v$  for all functions  $\phi$  and  $\psi$  on  $B$  satisfying the boundary condition (1). That is,  $\mathcal{L}$ , under the boundary condition (1), is a self-adjoint operator with respect to the inner product  $(\cdot, \cdot)_v$ . Appendix B discusses this  $v$  symmetry for higher-dimensional diffusions.

The diffusion process is *time reversible* if it is statistically the same when time runs backwards (which requires that the chain be conservative and stationary). A stationary diffusion with equilibrium density  $v$  and the boundary conditions described is time reversible if and only if it is  $v$  symmetric [21]. However, a diffusion with destroying (i.e., a nonconservative diffusion) can also be  $v$  symmetric for some  $v$ .

Given the diffusion coefficient  $D$  and a positive function  $v$  on  $B$ , there is a unique choice of the drift function  $\mu$  for which the diffusion is  $v$  symmetric [21,24,25]. Writing  $v$  in the form  $v = \alpha \exp(-u)$ , where  $\alpha$  is a normalizing constant and  $u$  is a twice continuously differentiable function on  $B$ , the condition on the drift is

$$\mu = \frac{\partial D}{\partial x} - D \frac{\partial u}{\partial x}$$

or, equivalently,

$$\tilde{\mu} = -D \frac{\partial u}{\partial x}.$$

That is,  $v$  symmetry is equivalent to the drift function  $\tilde{\mu}$  being the negative gradient, scaled by  $D$ , of a potential function  $u$ .

Given a  $v$ -symmetric diffusion process  $\hat{W}$ , a sequence of Markov chains  $\{\hat{X}^N\}_{N \in \mathbb{N}}$  is said to be *associated* with  $\hat{W}$  if (i)  $\hat{X}^N$  converges in distribution to  $\hat{W}$  as  $N \rightarrow \infty$  and (ii)  $\hat{X}^N$  is  $\mathcal{V}$  symmetric, where  $\mathcal{V}$  is a discretization of  $v$ .

Let us find a sequence of Markov chains associated with a one-dimensional  $v$ -symmetric diffusion process  $\hat{W}$  on  $[0, L_c]$  such that  $v(x) = \exp[-u(x)]$  for some energy function  $u(x)$ . Assume that the diffusion coefficient is  $D(x) > 0$ . Since the process is  $v$  symmetric, the infinitesimal drift  $\mu(x)$  is given by

$$\mu(x) = \frac{dD(x)}{dx} - D(x) \frac{du(x)}{dx}. \quad (2)$$

Consider the channel being divided into sections of length  $\Delta x$ , where  $\Delta x = L_c/N$  is the space discretization parameter. Let  $\mathcal{V}_i = \exp(-U_i)$ , where  $U_i = u(i\Delta x)$ . We will specify a family of  $\mathcal{V}$ -symmetric birth-death Markov processes  $\hat{X}^N$ , so that as  $N \rightarrow \infty$ , the processes converge to  $\hat{W}$  in distribution. The processes are discrete in space. The remainder of this section considers a discrete-time model, but it is straightforward to adapt the procedure for a continuous-time model. Let the time discretization  $\Delta t$  be such that as  $\Delta x, \Delta t \rightarrow 0$ ,

$$\frac{(\Delta x)^2}{\Delta t} \rightarrow G,$$

where

$$G \geq 3 \max_{x \in [0, L_c]} 2D(x).$$

The  $\mathcal{V}$ -symmetry condition (see Sec. III) is that the transition probabilities  $p_{ij}$  satisfy

$$\exp(-U_i)p_{i,j} = \exp(-U_j)p_{j,i} \quad (3)$$

for  $i, j \in \{1, \dots, N\}$ . Equation (3) is trivially satisfied when  $j = i$ . For  $j \in \{i-1, i+1\}$ , Eq. (3) is equivalent to

$$\frac{p_{i,j}}{p_{j,i}} = \frac{\exp(-U_j)}{\exp(-U_i)} = \frac{\exp[-\frac{1}{2}(U_j - U_i)]}{\exp[-\frac{1}{2}(U_i - U_j)]}. \quad (4)$$

For  $i \in \{1, \dots, N\}$  and  $j \in \{i-1, i+1\}$  let

$$p_{i,j} = \frac{\Delta t}{(\Delta x)^2} \frac{D_i + D_j}{2} \exp\left(-\frac{1}{2}(U_j - U_i)\right), \quad (5)$$

where  $D_i = D(i\Delta x)$ , and let

$$p_{i,i} = 1 - (p_{i,i+1} + p_{i,i-1}). \quad (6)$$

Notice that  $\frac{\Delta t}{(\Delta x)^2}$  must be small enough to keep the one-step transition probabilities between 0 and 1, which is why a lower bound was required on  $G$ . Then Eq. (4) is satisfied, so the discrete-time, discrete-space Markov process  $\hat{X}^N$  with transition probabilities  $(p_{i,j})$  is  $\mathcal{V}$  symmetric as desired.

The one-step transition probabilities defined by Eqs. (5) and (6) do not make use of the original diffusion's drift explicitly. Nevertheless, the drift of the sequence of Markov chains converges to the drift  $\mu$  of the diffusion process, owing to Eq. (2) and the symmetry of the processes.

To check convergence to the original diffusion process, the main task is to check that the local drift and variance per unit time of the discrete processes converge to the drift function  $\mu$  and twice the diffusion function,  $2D$ , of the original diffusion process, respectively. (A rigorous proof of convergence in the distribution for random processes requires defining continuous-time versions of the discrete processes—for example, by linear interpolation—and checking conditions for tightness of their probability measures in path space. See, for example, [26–28] for details.)

So it needs to be shown that  $w(x) = \mu(x)$  and that  $\eta(x) = 2D(x)$ , where  $w(x)$  and  $\eta(x)$  are the limiting infinitesimal mean and variance per unit time, respectively. This can be easily checked from the first and second moments ( $w_i^1$  and  $w_i^2$ , respectively) of the unscaled jumps of the Markov chain from site  $i$ —i.e., from

$$w(x) = \lim_{\substack{\Delta x, \Delta t \rightarrow 0 \\ i\Delta x \rightarrow x}} \frac{\Delta x}{\Delta t} w_i^1, \quad (7)$$

$$\eta(x) = \lim_{\substack{\Delta x, \Delta t \rightarrow 0 \\ i\Delta x \rightarrow x}} \frac{(\Delta x)^2}{\Delta t} [w_i^2 - (w_i^1)^2], \quad (8)$$

where

$$w_i^1 = p_{i,i+1} - p_{i,i-1}, \quad (9)$$

$$w_i^2 = p_{i,i+1} + p_{i,i-1}. \quad (10)$$

Therefore, the sequence of Markov chains converges in distribution to the original diffusion process as claimed.

## V. NONINTERACTING STEADY-STATE MODELS

This section continues to move towards a model with interacting ions by considering the simplest models with multiple ions. Namely, the ions behave independently, each according to a single-ion model of the type discussed previously. We also switch to taking the discrete-state models to be in continuous time, because it naturally leads to only one ion moving at a time, leading to a much smaller number of possible transitions. First a closed single-ion model is specified, then a closed noninteracting model is specified, and finally an open noninteracting model is derived as the infinite ion limit of the closed model. The equilibrium distribution of the open noninteracting model is expressed in terms of the internal energy of the corresponding state configuration, which, in the terminology of statistical mechanics, is a grand canonical ensemble [29]. The statistical equivalence of left-right and right-left *trans* paths for any ion holds for the models of this section, because the statistical behavior of each ion in the channel follows a single-ion model of the type considered earlier.

### A. Closed single-ion model

Let  $L_c$  be the length of the channel, and let  $u(x)$  be the energy of the ion when it is located at  $x \in [0, L_c]$ , which can include the energy due to fixed electric potentials, image charges, and Born energy, for example. For  $x \in [0, L_c]$ , let  $D(x)$  be the diffusion coefficient. Let space be discretized by  $\Delta x = \frac{L_c}{N}$ , and let  $U_i = u(i\Delta x)$  and  $D_i = D(i\Delta x)$  for  $i \in \{0, \dots, N+1\}$ . The ion follows a conservative Markov chain  $X$  on  $\{0, \dots, N+1\}$ , as described in Sec. II, but operating in continuous time. Thus, transition rates  $(q_{i,j})$  will be specified, rather than transition probabilities  $(p_{i,j})$ .

Given that the process (without scaling) is in state  $i$ , its infinitesimal drift is  $q_{i,i+1} - q_{i,i-1}$  and its infinitesimal variance per unit time is  $q_{i,i+1} + q_{i,i-1}$ . These expressions match those on the right-hand sides of Eqs. (9) and (10) with  $p$ 's replaced by  $q$ 's. Therefore, the construction of the associated discrete-state processes in Sec. IV carries over to continuous time, yielding the following choice of transition rates, for some positive constants  $M$ ,  $\lambda_L$ , and  $\lambda_R$ . For  $|i-j|=1$ ,  $i \neq \{0, N+1\}$ ,

$$q_{i,j} = \frac{D_i + D_j}{2} e^{-(U_j - U_i)/2}, \quad (11)$$

$$q_{0,1} = \frac{\lambda_L D_0 + D_1}{M} e^{-(U_1 - U_0)/2}, \quad (12)$$

$$q_{N+1,N} = \frac{\lambda_R D_{N+1} + D_N}{M} e^{-(U_N - U_{N+1})/2}, \quad (13)$$

and  $q_{i,j} = 0$  for all other  $i \neq j$ . The diagonal of the transition rate matrix is given by

$$q_{i,j} = -(q_{i,i-1} + q_{i,i+1}),$$

except for  $q_{0,0} = -q_{0,1}$  and  $q_{N+1,N+1} = -q_{N+1,N}$ . At this point  $M$  is just a parameter value, but later on it will represent the number of ions. The constants  $M$ ,  $\lambda_L$ , and  $\lambda_R$  affect the entrance rates from the baths into the channel, as can be observed in Eqs. (12) and (13). As indicated in Sec. IV, this Markov process  $X$  is reversible, its scaled limit corresponds to an electrodiffusion process with diffusion coefficient  $D(x)$  and drift vector field  $\mu(x)$ , and its equilibrium distribution is a discretized version of the equilibrium distribution of the limit diffusion.

The equilibrium distribution  $\pi \in \mathbb{R}^{N+2}$  is of the Boltzmann type—i.e.,

$$\pi = \frac{1}{\alpha} \left( \frac{M}{\lambda_L} e^{-U_0}, e^{-U_1}, \dots, e^{-U_N}, \frac{M}{\lambda_R} e^{-U_{N+1}} \right), \quad (14)$$

where  $\alpha$  is a positive normalizing constant given by

$$\alpha = \frac{M}{\lambda_L} e^{-U_0} + e^{-U_1} + \dots + e^{-U_N} + \frac{M}{\lambda_R} e^{-U_{N+1}}. \quad (15)$$

The reversibility of  $X$  can indeed be verified by directly checking the detailed balance equations  $\pi_i q_{i,j} = \pi_j q_{j,i}$  for all  $i, j \in \{0, \dots, N+1\}$ .

### B. Closed noninteracting model

Given an integer  $M \geq 1$ , a closed model of  $M$  noninteracting ions is now considered, where each of the ions behaves according to the closed single-ion model just described. Let  $n_i \in \{0, \dots, M\}$  be the number of ions at site  $i$ , and let  $\vec{n} = (n_0, \dots, n_{N+1})$ , where  $n_0 + \dots + n_{N+1} = M$ . Since the ions are assumed to be independent, the joint equilibrium distribution of the ions, denoted by  $\Pi$ , can be obtained from the equilibrium distribution of the single-ion model (14) as

$$\begin{aligned} \Pi(\vec{n}) &= \binom{M}{n_0 \dots n_{N+1}} (\pi_0)^{n_0} \dots (\pi_{N+1})^{n_{N+1}} \\ &\stackrel{(a)}{=} \left( \frac{M!}{n_0! \dots n_{N+1}!} \right) \\ &\quad \times \frac{\left( \frac{M}{\lambda_L} e^{-U_0} \right)^{n_0} (e^{-U_1})^{n_1} \dots (e^{-U_N})^{n_N} \left( \frac{M}{\lambda_R} e^{-U_{N+1}} \right)^{n_{N+1}}}{\left( \frac{M}{\lambda_L} e^{-U_0} + e^{-U_1} + \dots + e^{-U_N} + \frac{M}{\lambda_R} e^{-U_{N+1}} \right)^M}, \end{aligned} \quad (16)$$

where (a) follows from Eqs. (14) and (15) and the expression for multinomial coefficients:

$$\binom{i}{j_0 \dots j_a} = \frac{i!}{j_0! \dots j_a!}.$$

The rates at which ions jump from one site to the other in this model are proportional to the corresponding transition rates between sites of the individual ion processes. The proportionality constants are the number of ions at the site where the jump originates—i.e.,

$$q_{(n_1, \dots, n_i, n_j, \dots, n_N), (n_1, \dots, n_{i-1}, n_j+1, \dots, n_N)} = n_i q_{i,j},$$

where  $q_{i,j}$  are the transition rates of the single-ion process, given by Eqs. (11) and (12). It is easy to check that these transition rates are  $\Pi$  symmetric and that they correspond to a conservative process; hence, the model is reversible. Due to the reversibility of the process, the equivalence in distribution of the time-reversed *trans* paths holds in this model as well.

Denote the total number of ions inside the channel (so not in the baths) by  $a = n_1 + \dots + n_N$  and let  $\hat{n} = (n_1, \dots, n_N)$ . The marginal distribution of the ions inside the channel, denoted by  $\hat{\Pi}$ , can be obtained from Eq. (14) as

$$\begin{aligned} \hat{\Pi}(\hat{n}) &= \binom{M}{n_1 \dots n_N M - a} (\pi_1)^{n_1} \dots (\pi_N)^{n_N} (\pi_0 + \pi_{N+1})^{M-a} \\ &\stackrel{(a)}{=} \frac{(M-a+1)(M-a+2) \dots (M-1)M}{M^a} \frac{(e^{-U_1})^{n_1}}{n_1!} \dots \\ &\quad \times \frac{(e^{-U_N})^{n_N}}{n_N!} \rho^a \left( 1 + \frac{1}{M} \rho (e^{-U_1} + \dots + e^{-U_N}) \right)^{-M}, \end{aligned} \quad (17)$$

where (a) follows by substituting Eqs. (14) and (15), rearranging terms, and

$$\rho := \left( \frac{e^{-U_0}}{\lambda_L} + \frac{e^{-U_{N+1}}}{\lambda_R} \right)^{-1}. \quad (18)$$

### C. Open noninteracting model

A reversible open noninteracting model is now obtained by taking  $M \rightarrow \infty$  in the closed model just described. Notice that as  $M \rightarrow \infty$ , the entrance rates  $q_{0,1}$  and  $q_{N+1,N}$  from the baths into the channel of the closed single-ion model, given by Eqs. (12) and (13), converge to zero. However, the other transition rates, given by Eq. (11), remain the same. The equilibrium distribution for one individual ion, given by Eq. (14), converges to

$$\pi \rightarrow \left( \frac{\rho}{\lambda_L} e^{-U_0}, 0, \dots, 0, \frac{\rho}{\lambda_R} e^{-U_{N+1}} \right), \quad (19)$$

which indicates that for large  $M$ , the ion will tend to stay out of the channel. However, since there are many ions in the closed model, the channel need not be empty most of the time.

The equilibrium distribution of the limiting open model, denoted by  $\mathcal{P}$ , is obtained from the marginal distribution of ions inside the channel of the closed model (17) as

$$\begin{aligned} \mathcal{P}(\hat{n}) &= \lim_{M \rightarrow \infty} \hat{\Pi}(\hat{n}) = \left( \frac{(\rho e^{-U_1})^{n_1}}{n_1!} \exp(-\rho e^{-U_1}) \right) \dots \\ &\quad \times \left( \frac{(\rho e^{-U_N})^{n_N}}{n_N!} \exp(-\rho e^{-U_N}) \right), \end{aligned}$$

which is the product distribution corresponding to  $N$  independent Poisson random variables with parameters  $\rho \exp(-U_i)$  for  $i \in \{1, \dots, N\}$ . On average, there are  $\rho[\exp(-U_1)$

$+\dots + \exp(-U_N)]$  ions inside the channel in steady state, and this number can be tailored to whatever desired value through  $\rho$  by scaling  $\lambda_R$  and  $\lambda_L$ , as can be noticed from Eq. (18).

The equilibrium distribution of this open model can be expressed as a grand canonical ensemble [29] with an internal energy function  $V$ , as follows:

$$\mathcal{P}(\hat{n}) = \frac{1}{\hat{\alpha} n_1! \dots n_N!} e^{-V(\hat{n})},$$

where the internal energy function is given by

$$V(\hat{n}) = \sum_{i=1}^N n_i U_i$$

and  $\hat{\alpha}$  is a constant chosen so that  $\mathcal{P}(\hat{n})$  is a probability distribution. The constant  $\hat{\alpha}$ , also called the partition function, is given by

$$\hat{\alpha} = \sum_{\substack{j, n_1, \dots, n_N \geq 0: \\ n_1 + \dots + n_N = j}} \frac{\rho^j e^{-V(\hat{n})}}{n_1! \dots n_N!} = \exp[\rho(e^{-U_1} + \dots + e^{-U_N})].$$

The transitions rates in the closed model involving an ion already in the channel do not depend on  $N$  and thus will be the same in the limiting open model. Given a state  $\hat{n}$  and  $0 \leq i, j \leq N+1$  with  $|i-j|=1$ , let  $\hat{n}^{i,j}$  denote the state obtained from state  $\hat{n}$  by transferring an ion from site  $i$  to site  $j$ . For example, if  $1 \leq i, j \leq N$ ,

$$\hat{n}^{ij} = (n_1, \dots, n_i - 1, \dots, n_j + 1, \dots, n_N),$$

$$\hat{n}^{1,0} = (n_1 - 1, n_2, \dots, n_N),$$

$$\hat{n}^{N+1,N} = (n_1, \dots, n_{N-1}, n_N + 1).$$

For  $1 \leq i \leq N$ ,  $0 \leq j \leq N+1$ , and  $|i-j|=1$ , the following transition rates for the open model are the same as those for the closed model:

$$q_{\hat{n}, \hat{n}^{i,j}} = n_i q_{i,j} = n_i \frac{D_i + D_j}{2} e^{-(U_j - U_i)/2}. \quad (20)$$

It remains to specify transition rates for ions entering the channel. In the closed system there are  $M\pi_0$  ions at the left bath on average and each one enters the channel at a rate  $q_{0,1}$ . Therefore, in the open model, independent ions enter the channel from the left bath at a (total) rate given by

$$q_{\hat{n}, \hat{n}^{0,1}} = \lim_{M \rightarrow \infty} M \pi_0 q_{0,1} = \theta_L \rho e^{-U_0} \frac{D_0 + D_1}{2} e^{-(U_1 - U_0)/2}, \quad (21)$$

where (a) follows from Eqs. (12) and (19) and  $\theta_L = 1$ . (Later we consider different choices of  $\theta_L$ , leading to a nonreversible model.) Similarly, independent ions enter the channel from the right bath at a (total) rate given by

$$q_{\hat{n},\hat{n}^{N+1,N}} = \lim_{M \rightarrow \infty} M \pi_{N+1} q_{N+1,N} \\ = \theta_R \rho e^{-U_{N+1}} \frac{D_{N+1} + D_N}{2} e^{-(U_N - U_{N+1})/2}, \quad (22)$$

where, for now,  $\theta_R = 1$ . It can be easily checked that the transition rates of this open model (with  $\theta_L = \theta_R = 1$ ) given by Eqs. (20)–(22) are  $\mathcal{P}$  symmetric. Therefore this conservative process is reversible. Intuitively speaking, the reversibility is inherited, in the limit, from the closed model.

We pause to make some observations about the open model. The rates for transitions which preserve the number of ions in the system can be expressed in terms of the difference in internal energy of the system. Specifically, if  $1 \leq i, j \leq N$  with  $|i - j| = 1$ , then

$$q_{\hat{n},\hat{n}^{i,j}} = n_i \frac{D_i + D_j}{2} e^{-[V(\hat{n}^{i,j}) - V(\hat{n})]/2}. \quad (23)$$

Equation (23) does not hold for the transitions in which an ion enters or exits the system.

The only transition rates for the open model that depend on  $\rho$  are the entrance rates for new ions, given by Eqs. (21) and (22). So far, we have assumed  $\theta_L = \theta_R = 1$ . But if  $\theta_L = \theta_R = \theta$  for any positive constant  $\theta$ , then the constant  $\theta$  can be incorporated into the constant  $\rho$ , so that the resulting process is reversible whenever  $\theta_L = \theta_R$ .

The constants  $\lambda_L$  and  $\lambda_R$  do not separately appear in the transition rate for the open system, though they do influence  $\rho$ .

The reason is, intuitively, that a smaller value of  $\lambda_L$  in the closed model leads to a larger number of ions in the left bath, which tends to offset the small value of  $\lambda_L$ . Moreover, the ratio of the entrance rate on the left to the entrance rate on the right is given by

$$\frac{q_{\hat{n},\hat{n}^{0,1}}}{q_{\hat{n},\hat{n}^{N+1,N}}} = \frac{\theta_L}{\theta_R} \frac{D_0 + D_1}{D_N + D_{N+1}} e^{-[(U_0 + U_1)/2 - (U_N + U_{N+1})/2]}.$$

Thus, as long as  $\theta_L = \theta_R$ , the ratio is fixed by the diffusion coefficient function  $D$  and potential function  $u$ .

Due to the reversibility of the process, the equivalence in distribution of the time-reversed *trans* paths holds in this model. Furthermore, the equivalence holds even if the system is not in equilibrium or if  $\theta_R \neq \theta_L$ , because each ion in the channel independently follows an  $e^{-U_i}$ -symmetric Markov process. Since the diffusion limit of the single-ion processes corresponds to an electrodiffusion process, it follows from the independence between ions that the diffusion limit of this open noninteracting model is a Nernst-Planck electrodiffusion process with diffusion coefficient  $D(x)$  and drift  $\mu(x)$ .

## VI. INTERACTING IONS IN REVERSIBLE EQUILIBRIUM

Building on the open noninteracting model of the previous section, in this section a reversible open interacting model is suggested by adding an interaction energy term to internal energy. It is assumed that the interaction is present only inside the channel, not in the baths. This models the

case that the baths are large and rapidly mixing. The interaction that incoming ions experience inside the channel causes the entrance rates from the baths into the channel to depend on the channel state. A special case is considered by assuming that there is a neutral (interaction-free) lobby at each end of the channel to which ions jump from the baths. In this case, the entrance rates do not depend on the channel state.

Let  $\psi_{i,j}$  denote the interaction energy between an ion at site  $i$  and an ion at site  $j$ , which can be due to Coulomb or Lennard-Jones potentials, for example. The interaction energy function  $\psi_{i,j}$ , along with the energy function  $U_i$ , can also account for the effect of induced surface charges on the dielectric channel boundary, because the charge induced by a particular ion is proportional to the charge on the ion.

It is assumed that this interaction energy function is symmetric—i.e.,  $\psi_{i,j} = \psi_{j,i}$ . If  $\psi_{i,j} = 0$ , there is no interaction between ions located at site  $i$  and those at site  $j$ . The interaction is incorporated by including an interaction potential to the internal energy function, so that the internal energy function becomes

$$V(\hat{n}) = \sum_{i=1}^N n_i U_i + V_I(\hat{n}),$$

where  $V_I$  is the interaction potential defined by

$$V_I(\hat{n}) = \frac{1}{2} \sum_{\substack{i,j=1 \\ i \neq j}}^N n_i n_j \psi_{i,j} + \frac{1}{2} \sum_{i=1}^N n_i (n_i - 1) \psi_{i,i}.$$

The first summation in  $V_I$  corresponds to the interaction energy between ions at different sites, and the second summation corresponds to the interaction energy between ions at the same site. Multiple ions can be discouraged from being located simultaneously at the same site by letting

$$\psi_{i,i} \gg \max \left\{ \max_{i \in \{1, \dots, N\}} \{U_i\}, \max_{i,j \in \{2, \dots, N-1\}, i \neq j} \{\psi_{i,j}\} \right\}$$

for  $i \in \{2, \dots, N-1\}$ . This is appropriate if the channel is so narrow that ions cannot pass each other inside the channel.

Given two distinct states  $\hat{n}$  and  $\hat{n}'$ , the transition rate  $q_{\hat{n},\hat{n}'}$  for the open interacting model is taken to be given by

$$q_{\hat{n},\hat{n}'} = q_{\hat{n},\hat{n}'}^o e^{-[V_I(\hat{n}') - V_I(\hat{n})]/2}, \quad (24)$$

where  $q_{\hat{n},\hat{n}'}^o$  denotes the transition rates for the open noninteracting model of the previous section. The reversibility of the open noninteracting model implies that

$$\mathcal{P}^o(\hat{n}) q_{\hat{n},\hat{n}'}^o = \mathcal{P}^o(\hat{n}') q_{\hat{n}',\hat{n}}^o. \quad (25)$$

It follows immediately from Eqs. (24) and (25) that the open interacting model is reversible with equilibrium distribution given by  $\mathcal{P}(\hat{n}) = \mathcal{P}^o(\hat{n}) \exp[-V_I(\hat{n})]/Z$ , where  $Z$  is a normalizing constant.

More explicitly, the transition rates for the open interacting model are given as follows. The rates for transitions preserving the number of ions in the channel are given by

$$q_{\hat{n},\hat{n}^i,j} = n_i \frac{D_i + D_j}{2} e^{-[V(\hat{n}^i,j) - V(\hat{n})]/2} = n_i \frac{D_i + D_j}{2} e^{-(U_j - U_i)/2} \times \exp \left[ -\frac{1}{2} \left( (n_i - 1 - n_i) \psi_{i,j} + n_i \psi_{j,j} - (n_i - 1) \psi_{i,i} + \sum_{\substack{a=1 \\ a \neq i,j}}^N n_a (\psi_{a,j} - \psi_{a,i}) \right) \right] \quad (26)$$

for  $1 \leq i, j \leq N$  and  $|i - j| = 1$ . The rates for transitions involving an ion exiting the channel are given by

$$q_{\hat{n},\hat{n}_{10}} = n_1 \frac{D_1 + D_0}{2} \exp \left[ -\frac{1}{2} \left( U_0 - U_1 - (n_1 - 1) \psi_{1,1} - \sum_{i=2}^N n_i \psi_{1,i} \right) \right]$$

and

$$q_{\hat{n},\hat{n}_{N+1,N}} = n_N \frac{D_N + D_{N+1}}{2} \exp \left[ -\frac{1}{2} \left( U_{N+1} - U_N - (n_N - 1) \psi_{N,N} - \sum_{i=1}^{N-1} n_i \psi_{N,i} \right) \right].$$

Finally, the rates for transitions involving an ion entering the channel are given by

$$q_{\hat{n},\hat{n}_{01}} = \theta_L \rho e^{-U_0} \frac{D_0 + D_1}{2} \exp \left[ -\frac{1}{2} \left( U_1 - U_0 + \sum_{i=1}^N n_i \psi_{1,i} \right) \right]$$

and

$$q_{\hat{n},\hat{n}_{N+1,N}} = \theta_R \rho e^{-U_{N+1}} \frac{D_{N+1} + D_N}{2} \times \exp \left[ -\frac{1}{2} \left( U_N - U_{N+1} + \sum_{i=1}^N n_i \psi_{N,i} \right) \right],$$

where, for now,  $\theta_L = \theta_R = 1$ .

One motivation for the choice (24) for transition rates is that, if  $\psi_{i,j} \equiv 0$ , the rates reduce to those of the noninteracting model discussed in Sec. V C. A second motivation is based on the discretization procedure of Sec. IV, which models the motion of a single ion. Specifically, Eq. (5) is used to define transition probabilities, or transition rates, given an energy function  $u$  and a diffusion function  $D$ , for a discrete space model for single-ion motion. Those transition rates are a function of the energy difference between the sites involved in the jump. The diffusion limit of that discrete-space model has a drift function given by  $\tilde{\mu}(x) = -D(x) \frac{du(x)}{dx}$  and diffusion function  $D(x)$ . We can identify  $V$  as a function of the position of one ion with all the other ions fixed with the function  $U$  of Sec. IV. Then, when the system state in this interacting model is  $\hat{n}$ , the jump of a single ion from site  $i$  to site  $j$  causes an energy difference  $V(\hat{n}^i,j) - V(\hat{n})$ . Comparing Eqs. (26) with (5) one can infer that the local drift experienced by

an individual ion in the diffusion limit of this open interacting model is proportional to the gradient of the internal energy, with the other ions considered to be fixed, times the diffusion coefficient. This interpretation relies on the fact that in these continuous-time models only one ion jumps at a time.

Reversibility of the model means that if the model operating in statistical equilibrium were filmed, then the same statistical picture would result if the film were run backwards in time. An observer might make a list of left-right *trans* paths as follows. Each time an ion enters from the left, the observer tracks the timed path of the ion. If the ion exits to the right, the path is appended to the list of observed left-right *trans* paths. If the ion exits to the left, the record for that ion is discarded. Similarly, an observer could make a list of right-left *trans* paths. Due to the reversibility, the distribution of one of the left-right *trans* paths is the same as the distribution of one of the time-reversed right-left *trans* paths. This is true even though the ions interact with each other. Also, the observer will see left-right *trans* paths occurring at the same long-term rate as right-left *trans* paths. This is a consequence of reversibility and can also be thought of as a property inherited from a closed-channel model as the number of ions converges to infinity. In contrast, the rate of left-left *cis* paths (a *cis* path is traced by an ion exiting on the same side that it enters) need not equal the rate of right-right *cis* paths.

Throughout this section it was assumed that  $\theta_L = \theta_R = 1$ . As in the case of the open noninteracting model, the choice  $\theta_L = \theta_R = \theta$  for any  $\theta > 0$  is equivalent to  $\theta_L = \theta_R = 1$  and  $\rho$  replaced by  $\theta\rho$ , and in particular the model is reversible. In the next section we explore, through simulation, a model with  $\theta_L \neq \theta_R$ .

## VII. INTERACTING IONS IN NONREVERSIBLE EQUILIBRIUM

This section discusses the effects of some of the system parameters in this open interacting model and also investigates systems with  $\theta_L \neq \theta_R$  for which the equilibrium is not reversible. It is assumed that the ions jump from the baths into neutral lobbies that are part of the channel but where the ions do not experience interaction with other ions in the channel—i.e.,  $\psi_{1,j} = \psi_{N,j} = 0$  for  $j \in \{1, \dots, N\}$ .

The ions at the neutral lobbies can move farther into the channel where the ions experience an interaction with other ions, or they can leave the channel. A channel of length  $L_c = 1 \times 10^{-8}$  m is considered with a space-step size  $\Delta x = \frac{L_c}{N}$  and time-step size  $\Delta t = \frac{(\Delta x)^2}{2D}$ , where  $D$  is the space homogeneous diffusion coefficient, which is assumed to be  $1 \times 10^{-9}$  m<sup>2</sup>/s. For simplicity, in this example, we do not include the effect of induced surface charges on the dielectric channel boundary, but we stress that they are very important for accurate modeling [13], and in theory they can be incorporated into the pairwise interaction potential  $\psi$  and energy  $u$  due to the electric potential. Thus, it is assumed that the interaction energy is due to Coulomb potentials—i.e.,



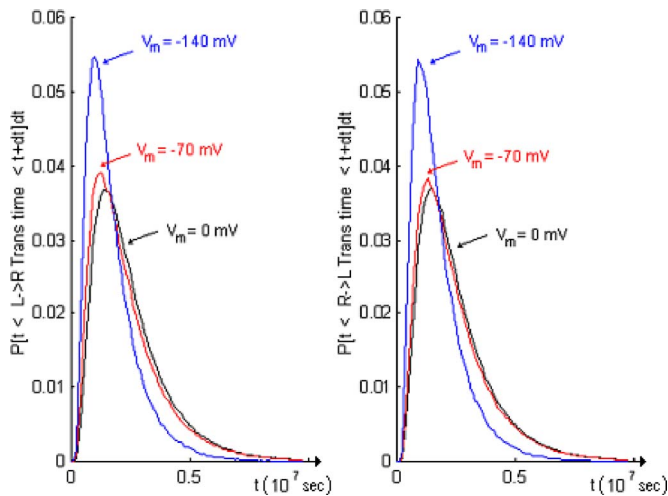


FIG. 4. (Color online) Effect of transmembrane potential on distribution of *trans* path duration,  $dt=1 \times 10^{-9}$  s.

$$\psi(x,y) = \frac{(Ze)^2}{4\pi\epsilon_r\epsilon_0 k_B T} \frac{1}{|x-y|},$$

where  $Z$  is the ion valence assumed to be  $+1$ ,  $e$  is the proton charge number  $\approx 1.602 \times 10^{-19}$  C,  $\epsilon$  is the electric permittivity of free space  $\approx 8.854 \times 10^{-12}$  F/m,  $\epsilon_r$  is the relative permittivity of the medium,  $k_B$  is Boltzmann's constant  $\approx 1.381 \times 10^{-23}$  J/K,  $T$  is the absolute temperature which is assumed to be 298 K, and  $x, y$  are the distances of the two ions from the left bath. Let the energy  $u$  be due to a linear electric potential

$$u(x) = \frac{Ze}{k_B T} \frac{V_m}{L_c} x,$$

where  $V_m$  is the transmembrane electric potential—i.e.,  $V_m = V_{\text{inside cell}} - V_{\text{outside cell}}$ , in units of volts. The relative permittivity is assumed to be that of water ( $\approx 80$ ), and the transmembrane electric potential is assumed to be  $-70 \times 10^{-3}$  V, unless indicated otherwise. We also took  $\lambda_L = \lambda_R = 0.5$ .

Figure 4 shows the distribution of the *trans* path duration under three different transmembrane potentials regimes. The left plot corresponds to the distribution of the left-to-right *trans* path duration, and the right plot corresponds to the distribution of the right-to-left *trans* path duration. It can be observed that the distributions of path duration of both types of *trans* paths are equivalent in all three regimes. This is expected because the entrance rates corresponding to reversibility are used. It can be also observed that larger transmembrane potentials, in absolute value, reduce the time it takes an ion to cross the channel. This is not surprising because larger transmembrane potentials generate larger driving forces on the ions.

Figure 5 shows the distribution of the *trans* path duration under three different Coulomb interaction strengths. Again, the left plot corresponds to the distribution of the left-to-right *trans* path duration, and the right plot corresponds to the distribution of the right-to-left *trans* path duration. Notice that the distributions of path duration of both types of *trans*

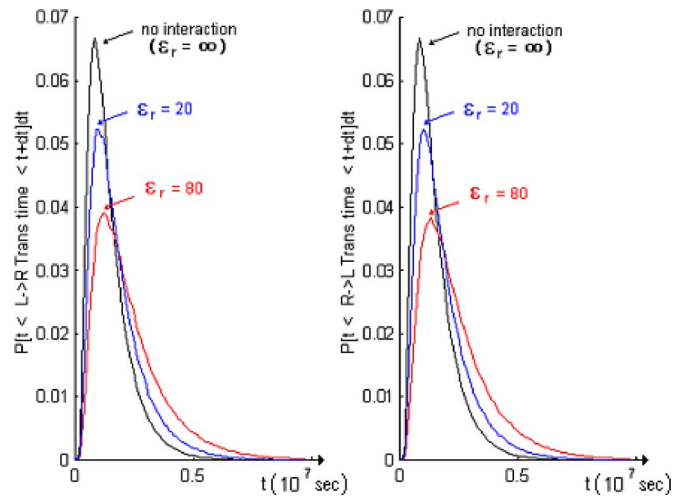


FIG. 5. (Color online) Effect of Coulomb interaction strength on the distribution of *trans* path duration,  $dt=1 \times 10^{-9}$  s.

paths are equivalent. The Coulomb interaction strength can be increased by reducing the relative permittivity, and it can be decreased by increasing the relative permittivity. The effect of changes in the relative permittivity on the viscosity of the medium, and hence on the diffusion coefficient, is neglected in this example. The limit  $\epsilon_r \rightarrow \infty$  would correspond to the case without Coulomb interaction. Relative permittivities below that of water would correspond to channels that are so narrow that there are gaps between water molecules. It can be observed that the Coulomb interaction strength does not have a monotonic effect on the time for ion crossing. At first glance it seems surprising that higher Coulomb interaction strength would yield faster transit times, but this is due to the fact that as the Coulomb interaction strength increases, ions are discouraged from entering the channel and the system looks more like a single-ion channel.

So far, it has been assumed that  $\theta_L = \theta_R$ , leading to reversibility. In particular, if  $\theta_L = \theta_R$ , the entrance rates at the right and left of the channel are such that, in the long run, the number of left-right *trans* paths per unit time equals the number of right-left *trans* paths per unit time. Even if  $\theta_L \neq \theta_R$ , the transition rates of the open noninteracting and interacting models are well defined. There is still an equilibrium probability distribution, even though it may be hard to describe, and if the system is initialized with the equilibrium probability distribution, it will be a stationary Markov process, remaining in the equilibrium distribution for all time. If  $\theta_L \neq \theta_R$ , then the open noninteracting model is not reversible, because the long-term rate of left-right *trans* paths would not equal the long-term rate of right-left *trans* paths. Therefore, if  $\theta_L \neq \theta_R$ , the symmetry condition (25) for the open noninteracting model is violated. It follows, therefore, that the open interacting model is also not reversible in the case  $\theta_L \neq \theta_R$ .

Intuitively, the case  $\theta_L \neq \theta_R$  means that the baths are so large, or else are actively pumped by some other channel, that the concentrations within the two baths are not in equilibrium as determined by the channel.

Figure 6 shows the distribution of the *trans* path duration under four different values for the pair  $(\theta_L, \theta_R)$ , as found by

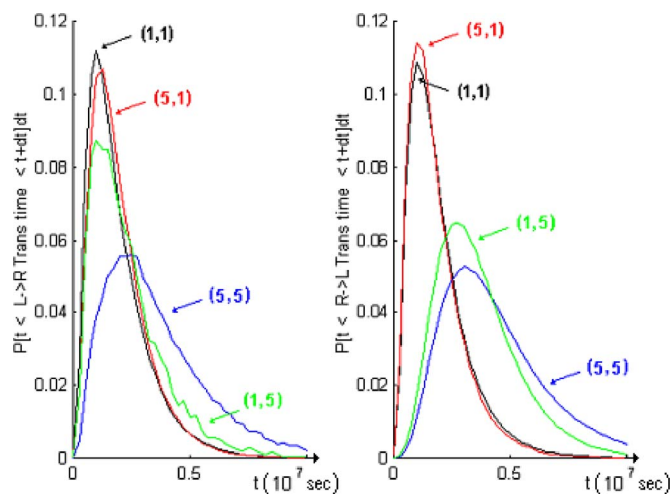


FIG. 6. (Color online) Effect of entrance rates on the distribution of *trans* path duration,  $dt=2.5 \times 10^{-9}$  s.

simulation. The left plot displays the distribution of the left-to-right *trans* path duration and the right plot displays the distribution of the right-to-left *trans* paths duration. In the two cases that  $\theta_L = \theta_R$ —namely, (1, 1) and (5, 5)—the distributions of path duration are the same in each direction. The case (5, 5) is the same as the case (1, 1), but with  $\rho$  increased by a factor of 5, corresponding to a higher mean concentration of ions. We observe in this simulation that the duration of transit times is longer for the larger  $\rho$ .

In the two cases that  $\theta_L \neq \theta_R$ —namely, (1, 5) and (5, 1)—the distributions of path duration in each direction are similar, but definitely not the same. In particular, in the case  $(\theta_L, \theta_R) = (1, 5)$ , so that there is a net flux of ions crossing from right to left across the channel (fighting against the transmembrane potential), the transit time from right to left is typically markedly longer than the transit time from left to right. It is conceivable that there is a choice of nontrivial interaction potential and  $\theta_L \neq \theta_R$  such that the duration of transit times is the same in each direction, but there is no reason to think that they should generally be exactly the same, and the simulations show that they definitely are not always the same.

### VIII. DISCUSSION

This paper points to the related concepts of reversibility and  $v$  symmetry of Markov processes to explain the equivalence of the transit time distribution, observed in ion channels. Such equivalence holds even when ion-ion interaction is taken into account, as long as the ratio of concentrations in the left and right baths is in an equilibrium determined by the channel.

We have used Markov models in this paper, even though there are long-standing objections in the literature to the use of Markov processes for the modeling of ion channels (cf., e.g., [30–36]), and recently these objections have found support by direct experimental evidence [37–40]. In particular, it is proposed that the holding time of a state, rather than having a memoryless distribution (i.e., the exponential distribu-

tion for continuous time or the geometric distribution for discrete time), should have a distribution with a heavy, power-law tail. For such a distribution, the longer an ion has been in a state, the longer it is likely to stay there. If the only aspect of non-Markov behavior is the distribution of the holding times, and not the selection mechanism for next states, then the equivalence of *trans* path distributions for a single ion described in Sec. III immediately carries over. If there is non-Markov behavior also in the selection mechanism for the next states, then the process can perhaps be embedded into a higher-dimensional Markov process. When we discussed interacting ions, we relied more heavily on the Markov assumption, because we described the dynamics using a potential function, and the potential function is a function of the state. If the process is not Markov, perhaps it would be for a large state space. For example, the state could include not only the position of an ion, but also its momentum or local speed. In the end, we (1) point out that reversibility, *per se*, is easier to discuss and characterize for Markovian processes, but it can also hold for general time-stationary random processes, and (2) we leave it for future research to determine whether our findings extend to non-Markov models of interacting ions.

Reversibility has been studied in various guises for at least 80 years. [The principle of microscopic reversibility was proposed by Tolman in 1924 (see [41]).] We suggest that reversibility, when present, may be worth preserving, when forming a discrete-state model from a continuous-state model. A method for such discretization is described in Sec. IV. Our motivation was to explicitly investigate a question related to reversibility—namely, whether transit times are equivalent in a nonreversible equilibrium with an ion-ion interaction. It would be interesting to know if there are any reasons related to numerical stability, for which reversibility should be preserved in discretizing a model. Perhaps the fact that the eigenvalues of reversible generators are real valued offers an advantage.

Reversibility, if it could be established for a given channel, could be helpful to experimentalists. In particular, if there is a significant *trans*-membrane potential, most of the paths beginning at one side of the channel may be *trans* paths, while most of the paths beginning at the other end may be *cis* paths. Thus, it may be easier to isolate the transit distribution by focusing measurement in one direction.

Accurately modeling transit times for ion channels is a part of the puzzle of understanding the speed of communication within biological organisms. The fact that transit times can be just as short for ions traversing against a potential as with a potential may offer insights for system level analysis.

### ACKNOWLEDGMENTS

We are thankful to Professor Eric Jakobsson for his suggestions. This work was supported in part by the National Science Foundation under Grant. No. ANR 99–80544.

### APPENDIX A: EQUIVALENCE OF *trans* PATHS

The proof of proposition III.1 is provided in this appendix. The proposition is renumbered A.1

*Proposition A.1.* For any  $\gamma \in \mathcal{S}_{LR}$ ,  $P_{LR}[\gamma] = P_{RL}[\gamma_{rev}]$ .  
*Proof.* Note that

$$P_{LR}[\gamma] = \frac{P^1[\tilde{\gamma}, T_{N+1} < T_0]^{(a)}}{P^1[T_{N+1} < T_0]} = \frac{P^1[\tilde{\gamma}]}{P^1[T_{N+1} < T_0]} \stackrel{(b)}{=} \frac{P^1[\tilde{\gamma}]}{\sum_{\gamma' \in \mathcal{S}_{LR}} P^1[\gamma']} \stackrel{(c)}{=} \frac{P^1[\gamma]}{\sum_{\gamma' \in \mathcal{S}_{LR}} P^1[\gamma']}, \quad (\text{A1})$$

where (a) follows because  $\tilde{\gamma}$  implies  $T_{N+1} < T_0$ ; (b) follows because all paths exit through one of the boundaries, so the probability of exiting through the right boundary is simply the sum over all those paths that exit through the right boundary; and (c) follows because  $P^1[\tilde{\gamma}] = P^1[\gamma] p_{N,N+1}$ , so that  $p_{N,N+1}$  in the numerator and denominator cancel each other out. Similarly, for  $\gamma \in \mathcal{S}_{RL}$ ,

$$P_{RL}[\gamma] = \frac{P^N[\gamma]}{\sum_{\gamma' \in \mathcal{S}_{RL}} P^N[\gamma']}. \quad (\text{A2})$$

Let

$$\mathcal{V}_i := \begin{cases} 1, & i = 1, \\ \frac{p_{1,2} p_{2,3} \cdots p_{i-2,i-1} p_{i-1,i}}{p_{i,i-1} p_{i-1,i-2} \cdots p_{3,2} p_{2,1}}, & i \in \{2, \dots, N\}. \end{cases} \quad (\text{A3})$$

Then  $\mathcal{V}_i p_{i,j} = \mathcal{V}_j p_{j,i}$  for all  $i, j \in \{1, \dots, N\}$ . This relation is known as  $\mathcal{V}$  symmetry [21] or as detailed balance [20]. If  $\hat{X}$  were conservative, then  $\mathcal{V}$  symmetry would imply that  $\mathcal{V}$  is proportional to the equilibrium distribution of  $\hat{X}$ , and  $\hat{X}$  would be a reversible process [20,42].

Thus, for all  $i, j \in \{1, \dots, N\}$ ,

$$\frac{\mathcal{V}_i}{\mathcal{V}_j} = \frac{p_{j,i}}{p_{i,j}}. \quad (\text{A4})$$

By the Markov property, the probability of a particular path  $\gamma$  of length  $m$ , given the initial state of the process is  $\gamma_0$ , can be expressed as

$$P^{\gamma_0}[\gamma] = p_{\gamma_0, \gamma_1} p_{\gamma_1, \gamma_2} \cdots p_{\gamma_{m-2}, \gamma_{m-1}} p_{\gamma_{m-1}, \gamma_m}. \quad (\text{A5})$$

Then,

$$\begin{aligned} \frac{P^1[\gamma]}{P^N[\gamma_{rev}]} &\stackrel{(a)}{=} \frac{p_{1, \gamma_1} p_{\gamma_1, \gamma_2} \cdots p_{\gamma_{m-2}, \gamma_{m-1}} p_{\gamma_{m-1}, N}}{p_{N, \gamma_{m-1}} p_{\gamma_{m-1}, \gamma_{m-2}} \cdots p_{\gamma_2, \gamma_1} p_{\gamma_1, 1}} \\ &= \frac{p_{1, \gamma_1} p_{\gamma_1, \gamma_2} \cdots p_{\gamma_{m-2}, \gamma_{m-1}} p_{\gamma_{m-1}, N}}{p_{\gamma_1, 1} p_{\gamma_2, \gamma_1} \cdots p_{\gamma_{m-1}, \gamma_{m-2}} p_{N, \gamma_{m-1}}} \\ &\stackrel{(b)}{=} \frac{\mathcal{V}_{\gamma_1} \mathcal{V}_{\gamma_2} \cdots \mathcal{V}_{\gamma_{m-1}} \mathcal{V}_N}{\mathcal{V}_1 \mathcal{V}_{\gamma_1} \mathcal{V}_{\gamma_2} \cdots \mathcal{V}_{\gamma_{m-1}} \mathcal{V}_{\gamma_{m-1}}} = \frac{\mathcal{V}_N}{\mathcal{V}_1}, \end{aligned} \quad (\text{A6})$$

where (a) follows from by Eq. (A5) and (b) from Eq. (A4). Let  $\alpha := \mathcal{V}_N / \mathcal{V}_1$ . Then, Eq. (A6) becomes

$$P^1[\gamma] = \alpha P^N[\gamma_{rev}]. \quad (\text{A7})$$

Thus,

$$\begin{aligned} P_{LR}[\gamma] &\stackrel{(a)}{=} \frac{P^1[\gamma]}{\sum_{\gamma' \in \mathcal{S}_{LR}} P^1[\gamma']} \stackrel{(b)}{=} \frac{\alpha P^N[\gamma_{rev}]}{\sum_{\gamma' \in \mathcal{S}_{LR}} \alpha P^N[\gamma'_{rev}]} \stackrel{(c)}{=} \frac{P^N[\gamma_{rev}]}{\sum_{\gamma' \in \mathcal{S}_{RL}} P^N[\gamma'_{rev}]} \\ &\stackrel{(d)}{=} P_{RL}[\gamma_{rev}], \end{aligned}$$

where (a) follows from Eq. (A1), (b) from Eq. (A7), (c) because the mapping of  $\gamma \in \mathcal{S}_{LR}$  to  $\gamma_{rev}$  is a one-to-one and onto mapping of  $\mathcal{S}_{LR}$  to  $\mathcal{S}_{RL}$ , and (d) from Eq. (A2).  $\square$

## APPENDIX B: SYMMETRIC DIFFUSIONS

The symmetry discussion presented in Sec. IV for one-dimensional diffusions is extended to higher-dimensional diffusions in this appendix.

Let  $B$  be an open connected subset of  $\mathbb{R}^m$ . An  $m$ -dimensional diffusion on  $B$  has a backwards generator which is a second-order differential operator of the form

$$\mathcal{L}\phi = \sum_{i,j} D_{ij} \frac{\partial^2 \phi}{\partial x_i \partial x_j} + \sum_i \mu_i \frac{\partial \phi}{\partial x_i},$$

such that  $D$  is a symmetric, positive-definite matrix-valued function on  $B$  and  $\mu$  is a vector field on  $B$ . The generator can be rewritten in a more symmetrical (as an operator) form as

$$\mathcal{L}\phi = \sum_i \frac{\partial}{\partial x_i} D_{i,j} \frac{\partial \phi}{\partial x_j} + \sum_i \tilde{\mu}_i \frac{\partial \phi}{\partial x_i},$$

where

$$\tilde{\mu}_i = \mu_i - \sum_j \frac{\partial D_{ij}}{\partial x_j}.$$

The vector field  $\mu$  specifies the infinitesimal drift of the process, and  $2D$  specifies the infinitesimal covariance of the process.

In addition, the behavior of the diffusion at the boundary  $\partial B$  of  $B$  must be specified, unless the diffusion cannot reach the boundary, such as if  $B = \mathbb{R}^m$ . Following Kent [21], we shall assume that the boundary behavior is a mixture of destroying and normal (relative to  $D^{-1}$ ) reflection at the boundary. Specifically, if  $\xi \in \partial B$ , the outward normal (relative to  $D^{-1}$ ) vector  $n(\xi)$  is the outward-pointing vector such that  $[n(\xi)]^T D^{-1}(\xi) v = 0$  for all vectors  $v$  tangent to  $\partial B$  at  $\xi$ , normalized so that  $[n(\xi)]^T D^{-1}(\xi) n(\xi) = 1$ . The boundary behavior is specified by the following condition for a function  $f$  on  $B$ :

$$\alpha f + \beta n \cdot \nabla f = 0 \quad \text{on } \partial B, \quad (\text{B1})$$

where  $\alpha$  and  $\beta$  are functions on  $\partial B$  with  $0 \leq \alpha \leq 1$  and  $\alpha + \beta \equiv 1$ . If  $\alpha \equiv 1$ , then the process is killed at the boundary and the process is not conservative. If  $\alpha \equiv 0$ , the process is reflected at the boundary and is therefore conservative.

Given a positive, twice continuously differentiable function  $v$  on  $B$ , the inner product of two functions  $\psi$  and  $\phi$  on  $B$  relative to  $v$  is defined as  $(\psi, \phi)_v = \int_B \psi \phi v dx$ . The diffusion

specified by  $\mathcal{L}$  and the boundary condition (B1) is said to be symmetric with symmetry density  $v$ , or simply  $v$  symmetric, if  $(\mathcal{L}\psi, \phi)_v = (\psi, \mathcal{L}\phi)_v$  for all functions  $\phi$  and  $\psi$  on  $B$  satisfying the boundary condition (B1). That is,  $\mathcal{L}$ , under the boundary condition (B1), is a self-adjoint operator with respect to the inner product  $(\cdot, \cdot)_v$ . Kolmogorov [24] initiated the study of symmetric diffusion processes. Ikeda and Watanabe ([25], pp. 275–281) gave an elegant description of Kolmogorov’s results in the framework of stochastic differential equations on manifolds. The paper of Kent [21] is readable without much knowledge of differential geometry and treats boundaries. Symmetric Markov processes are also central in the study of Dirichlet forms, where the Dirichlet form of a  $v$ -symmetric diffusion is the bilinear mapping  $(\psi, \phi) \rightarrow (\psi, -\mathcal{L}\phi)_v$  [43].

The diffusion process is *time reversible* if it is statistically

the same when time runs backwards (which requires that the chain be conservative and stationary). A stationary diffusion with equilibrium density  $v$  and the boundary conditions described is time reversible if and only if it is  $v$  symmetric [21]. However, a diffusion with destroying (i.e., a nonconservative diffusion) can also be  $v$  symmetric for some  $v$ .

Given the diffusion matrix  $D$  and a positive function  $v$  on  $B$ , there is a unique choice of the drift vector field  $\mu$  for which the diffusion is  $v$  symmetric [21,24,25]. Writing  $v$  in the form  $v = \alpha \exp(-u)$ , where  $\alpha$  is a normalizing constant and  $u$  is a twice continuously differentiable function on  $B$ , the condition on the drift is  $\mu = (\nabla \cdot D)^T - D \cdot \nabla u$  or, equivalently,  $\tilde{\mu} = -D \cdot \nabla u$ . That is,  $v$  symmetry is equivalent to the vector field  $\tilde{\mu}$  being the negative gradient, scaled by  $D$ , of a potential function  $u$ .

- 
- [1] B. Eisenberg, *Contemp. Phys.* **39**, 447 (1998).  
 [2] B. Hille, *Ionic Channels of Excitable Membranes*, 3rd ed. (Sinauer Associates, Sunderland, MA, 2001).  
 [3] K. Cooper, E. Jakobsson, and P. Wolynes, *Prog. Biophys. Mol. Biol.* **46**, 51 (1985).  
 [4] S. Chung and S. Kuyucak, *Biochim. Biophys. Acta* **1565**, 267 (2002).  
 [5] D. G. Levitt, *J. Gen. Physiol.* **113**, 789 (1999).  
 [6] R. J. Mashi, J. Schnitzer, and E. Jakobsson, *Biophys. J.* **81**, 2473 (2001).  
 [7] E. Jakobsson, *Methods* **14**, 342 (1998).  
 [8] S. Kuyucak, O. S. Andersen, and S. Chung, *Rep. Prog. Phys.* **64**, 1427 (2001).  
 [9] D. L. Ermak and J. A. McCammon, *J. Chem. Phys.* **69**, 1352 (1978).  
 [10] W. F. van Gasteren, H. J. C. Berendsen, and J. A. C. Rullmann, *Mol. Phys.* **44**, 69 (1981).  
 [11] W. F. van Gasteren and H. J. C. Berendsen, *Mol. Phys.* **45**, 637 (1982).  
 [12] S. Bek and E. Jakobsson, *Biophys. J.* **66**, 1028 (1994).  
 [13] B. Corry, S. Kuyucak, and S. Chung, *Biophys. J.* **78**, 2364 (2000).  
 [14] D. G. Levitt, *Biophys. J.* **37**, 575 (1982).  
 [15] D. G. Levitt, *Annu. Rev. Biophys. Chem.* **15**, 29 (1986).  
 [16] D. G. Levitt, *Biophys. J.* **59**, 271 (1991).  
 [17] R. S. Eisenberg, M. M. Klosek, and Z. Schuss, *J. Chem. Phys.* **102**, 1767 (1995).  
 [18] Z. Schuss, B. Nadler, and R. S. Eisenberg, *Phys. Rev. E* **64**, 036116 (2001).  
 [19] E. Jakobsson and S. Chiu, *Biophys. J.* **52**, 33 (1987).  
 [20] F. P. Kelly, *Reversibility and Stochastic Networks* (Wiley, Chichester, 1979).  
 [21] J. Kent, *Adv. Appl. Probab.* **10**, 819 (1978).  
 [22] J. Alvarez, Ph.D. thesis, University of Illinois at Urbana-Champaign, 2004.  
 [23] A. M. Berezhkovskii, M. A. Pustovoit, and S. M. Bezrukov, *J. Chem. Phys.* **119**, 3943 (2003).  
 [24] A. Komogorov, *Math. Ann.* **113**, 766 (1937).  
 [25] N. Ikeda and S. Watanabe, *Stochastic Differential Equations and Diffusion Processes* (North-Holland, Amsterdam, 1981).  
 [26] S. N. Ethier and T. G. Kurtz, *Markov Processes: Characterization and Convergence* (Wiley, New York, 1986).  
 [27] H. J. Kushner, *Approximation and Weak Convergence Methods for Random Processes* (MIT Press, Cambridge, MA, 1984).  
 [28] D. W. Stroock and S. R. S. Varadhan, *Multidimensional Diffusion Processes* (Springer-Verlag, New York, 1979).  
 [29] C. J. Thompson, *Mathematical Statistical Mechanics* (Princeton University Press, Princeton, 1972).  
 [30] L. S. Liebovitch and J. M. Sullivan, *Biophys. J.* **52**, 979 (1987).  
 [31] L. S. Liebovitch, J. Fischbarg, and J. P. Koniarek, *J. Membr. Sci.* **84**, 37 (1987).  
 [32] Z. J. Grzywna, L. S. Liebovitch, and Z. Siwy, *J. Membr. Sci.* **145**, 253 (1998).  
 [33] S. J. Korn and R. Horn, *Biophys. J.* **54**, 871 (1988).  
 [34] M. S. P. Sansom, F. G. Ball, C. J. Kerry, R. McGee, R. L. Ramsey, and P. N. Usherwood, *Biophys. J.* **56**, 1229 (1989).  
 [35] D. Petracchi, C. Ascoli, M. Barbi, S. Chillemi, M. Pellegrini, and M. Pellegrino, *J. Stat. Phys.* **70**, 393 (1993).  
 [36] J. Timmer and S. Klein, *Phys. Rev. E* **55**, 3306 (1997).  
 [37] A. Fuliński, Z. Grzywna, I. Mellor, Z. Siwy, and P. N. R. Usherwood, *Phys. Rev. E* **58**, 919 (1998).  
 [38] Z. Siwy and A. Fuliński, *Phys. Rev. Lett.* **89**, 158101 (2002).  
 [39] S. Mercik, K. Weron, and Z. Siwy, *Phys. Rev. E* **60**, 7343 (1999).  
 [40] S. Mercik, Z. Siwy, and K. Weron, *Physica A* **276**, 376 (2000).  
 [41] R. C. Tolman, *The Principles of Statistical Mechanics* (Oxford University Press, New York, 1938).  
 [42] J. R. Norris, *Markov Chains* (Cambridge University Press, Cambridge, England, 1999).  
 [43] M. Fukushima, *Dirichlet Forms and Markov Processes* (North-Holland, Amsterdam, 1980).